Int. J. Impact Engng Vol. 7, No. 3, pp. 307–325, 1988
Printed in Great Britain

0734–743X/88 $3.00 + 0.00
Pergamon Press plc

A SURVEY OF SHAPED-CHARGE JET PENETRATION MODELS

WILLIAM P. WALTERS*, W. J. FLIS and P. C. CHOU†‡
*Ballistic Research Laboratory, Aberdeen, MD 21005-5066, U.S.A. and †Dyna East Corporation, Philadelphia, Pennsylvania, U.S.A.

(*Received* 4 *September* 1987; *and in revised form* 8 *January* 1988)

Summary—A survey of analytical models that predict the penetration of a shaped-charge jet into various target materials is presented. This survey discusses the early (1940 vintage) Bernoulli-like models, the extension of these models to include particulated jets and variable velocity jets and models dealing with compressibility effects and jet drift. Penetration models associated with metallic rods are also presented, especially insofar as they relate to shaped-charge or explosively formed penetrator studies. Modern analytical penetration models, which are used by the authors, are also discussed. An extensive bibliography is included.

NOTATION

B_{max}	Brinell hardness of target
C.D.	charge diameter
D	rod diameter
E_l	energy in last part of projectile
g	gap distance between particles
g_0	empirical constant
H_D	dynamic hardness of target
H_0	height of interaction region
k_j	jet body shape factor
k_T	target body shape factor
l	jet length
L	rod length
M	jet mass
P	penetration depth
P_0	penetration depth at zero standoff
r_j	jet radius
S or S.O.	standoff
t	time
t_0	time for jet to reach the target
t_b	jet breakup time
T	time at end of penetration
U	penetration velocity
U_{min}	minimum penetration velocity
V	jet velocity
V_I	velocity at the top of the interaction region
V_{min}	minimum jet velocity
V_0	jet tip velocity
Y	target strength
α, β	empirical constants
γ	$(\rho_t/\rho_j)^{1/2}$
$d\xi$	incremental length of jet
λ	empirical constant
μ	dynamic viscosity
ρ_j or ρ_0	jet density
ρ_T or ρ_{To}	target density
σ_j	dynamic strength of jet
σ_p	dynamic strength of penetrator
σ_{SD}	stress state of deforming penetrator
σ_t	dynamic strength of target

Other specialized symbols are defined where they are first used.

‡Billings Professor of Mechanical Engineering, Drexel University, Philadelphia, U.S.A.

INTRODUCTION

Analytical models capable of predicting the penetration of the jets from shaped charges into a variety of target materials are extremely valuable to the terminal ballistician. Many disciplines are involved, since shaped-charge jets are used to penetrate or perforate armor, as well as rocks, soil, wood, ice and other non-metallic materials. These analytical models provide fast, analytical predictions where the time and resources available prohibit large hydrocode computer solutions. Also, the target may be monolithic or it may consist of several layers of different materials including air or liquids. For these reasons, analytical penetration expressions usually assume one-dimensional flow and employ other simplifying assumptions.

Early analytical penetration models (1940 vintage) were based on the Bernoulli principle. Later, empirical factors were introduced to account for particulation of the jet. Eventually, non-uniform-velocity (i.e. stretching) jets were incorporated into the models. Other authors included terms to account for jet and target strength effects, compressibility effects and the effects of jet drift, particle dispersion and particle tumbling. These models were based primarily on the Bernoulli principle or on a rod-type penetration model. Other models included transient effects based on a one-dimensional conservation of mass and momentum without recourse to the rod models or the Bernoulli concept.

SHAPED-CHARGE JET PENETRATION

Birkhoff *et al.* [1] and Hill *et al.* [2] developed a simple penetration theory from the hydrodynamic theory of impinging jets. This theory is documented in Refs [1–3].

Because of the hypervelocities associated with shaped charge jets, the pressures produced during jet–target impact far exceed the yield strength of most materials. Thus, to a first approximation, the strengths and viscosities of the jet and target materials can be neglected, allowing usage of the familiar hydrodynamic assumption of incompressible, inviscid fluid flow.

Consider a shaped-charge jet of length l, density ρ_j and velocity V penetrating a semi-infinite, monolithic target of density ρ_T. The penetration velocity is U, as shown in Fig. 1. The penetration is simpler when viewed from a system of co-ordinates moving with the penetration velocity U, as shown in Fig. 2. In this system the hole profile is fixed, and the jet moves to the right at a velocity $V - U$ and the target moves left at a velocity U. The pressure on the two sides of the interface between the jet and the target must be the same. Now, since the phenomenon is steady-state in this system of co-ordinates, Bernoulli's equation may be applied along the axial streamline so that

$$\frac{1}{2}\rho_j(V-U)^2 = \frac{1}{2}\rho_T U^2. \tag{1}$$

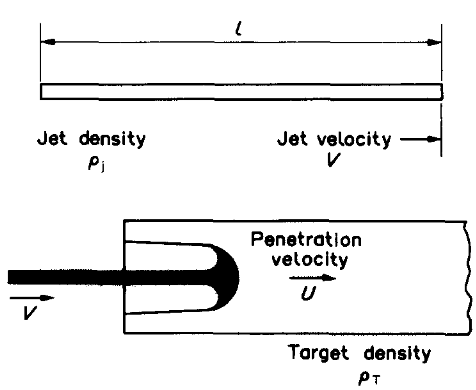

FIG. 1. Jet penetration.

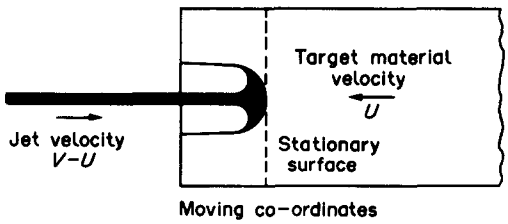

FIG. 2. Jet penetration with a co-ordinate system moving at the penetration velocity, U.

Figure 2 shows the jet being eroded while penetrating the target. Assuming that steady state is reached instantaneously and that the penetration ceases when the rear of the jet strikes the target, then the total penetration, P, is the penetration velocity times the penetration time or

$$P = U\frac{l}{V-U} \quad \text{or}$$
$$P = l(\rho_j/\rho_T)^{1/2} \quad \text{using equation (1).} \tag{2}$$

This simple equation indicates that the penetration is independent of the jet velocity. However, the rate at which the jet erodes and the final stretched length of jet depend on the jet velocity through the term l. Note that for real jets, l is a function of time.

There are several limitations to this simple theory. Firstly, after the last jet particle strikes the target, i.e. after the jet is consumed, the residual inertia of the penetrator may cause the hole to continue to grow in depth (and width). This additional depth has been called the secondary penetration [3] or afterflow. The depth of the crater when the jet vanishes is called the primary penetration.

Secondly, even the primary penetration is not predicted exactly, as effects other than density come into play. For example, a greater penetration into mild steel is observed than into armor steel, even though both have the same density. Moreover, more penetration into soft materials, such as lead, occurs than would be dictated by the density law. These results undoubtedly occur because material strength, strain, strain-rate dependence and other material properties are not included in the simple penetration model. These effects are especially important at low jet velocities, but less important at hypervelocities. In short, a density (and even a yield strength) is usually not sufficient to characterize a material.

Thirdly, for real jets, the average penetration into a given target increases, reaches a peak value and then decreases as the distance between the base of the charge and the target (the standoff) increases. Figure 3 illustrates a typical penetration–standoff curve for a shaped charge with a conical liner penetrating armor steel. This variation with standoff is not predicted by the simple penetration model, as discussed later.

If the jet is particulated (broken up) and separated such that the particles do not interfere with each other, the particles retain their velocity, $V - U$, and cross sectional area, A, until they impact the target, assuming the particles remain perfectly aligned and do not tumble, spread or diverge from the penetration axis.

Upon impact, the dynamic pressure produced by a jet particle can be approximated by dividing the total force by the total cross-sectional area the jet strikes.

Following Evans [4], the total force is given by the rate of change of momentum $\rho_j A(V-U)^2$ and the average pressure on the impact surface is $\rho_j(V-U)^2$. Equating this pressure to the pressure in the target material at the point of impact, from Bernoulli's equation, yields

$$\rho_j(V-U)^2 = \frac{1}{2}\rho_T U^2. \tag{3}$$

Comparison with equation (1) leads to

$$\lambda\rho_j(V-U)^2 = \rho_T U^2, \tag{4}$$

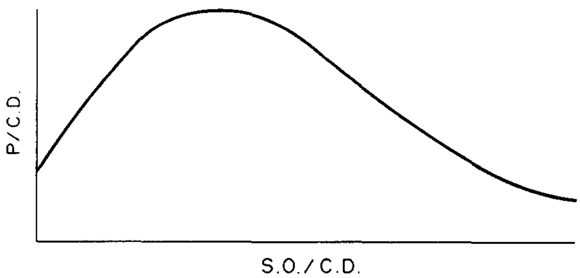

FIG. 3. Penetration–standoff curve for a conical liner.

where λ is a constant that equals one for a continuous jet and two for a particulated jet. ρ_j is then the average jet density including the gaps between particles. For jets particulated partially or particulated during the penetration process, $1 < \lambda < 2$. Then from equation (2) the ideal primary penetration becomes

$$P = l\left(\frac{\lambda\rho_j}{\rho_T}\right)^{1/2}. \tag{5}$$

This quantitative hydrodynamic theory of penetration by hypervelocity jets was developed by Hill, Mott, Pack and Evans (see [2], [4] and [5]) and independently by Pugh [6]. Additional details regarding the development of the hydrodynamic, hypervelocity penetration theory are given by Birkhoff *et al.* [1], Eichelberger [7], Birkhoff [8] and Ref. [3]. Birkhoff relates the parameter λ to the drag coefficient and calculates the penetration for a rotating jet.

This simple theory does not take into account jet velocity gradients, jet–target interactions, jet alignment, shock physics, compressibility effects, aerodynamic drag, variable-area jets, transient effects and jet–target material properties. References [5, 7] provide additional information regarding penetration theory and secondary penetration (or afterflow effects).

Other equations useful in penetration theory are, by definition,

$$P = \int U\,dt \quad \text{or} \quad U = \dot{P}, \tag{6}$$

where $\dot{P}$ denotes the derivative of P with respect to time, and

$$dl = (V - U)\,dt. \tag{7}$$

Equations (6) and (7) yield

$$P = \int \frac{U}{V - U}\,dl. \tag{8}$$

Early models attempted to improve the accuracy of the simple theory to better account for jet particulation (and spread) and standoff effects; these models were semi-empirical in nature. Let S denote the standoff and α be some constant depending on the jet velocity gradient; also, let β be a constant that determines the rate of jet spreading (dispersion). Then, for continuous (or very recently particulated) jets

$$P = P_0\frac{1 + \alpha S}{1 + \beta S}, \tag{9}$$

where P_0 is the penetration at zero standoff distance [1]. For fully particulated jets where $\lambda = 2$, the penetration may be given as

$$P = P'_0[\sqrt{2}(1 + \alpha S)^{1/2}/(1 + \beta S)], \tag{10}$$

where P'_0 is the value of P from equation (9) at $S = S_1$, where the jet breaks up [1]. This model assumes that the ratio of the effective jet length at some standoff S to that at $S = 0$ is $1 + \alpha S$.

Also, the ratio of the effective cross-sectional area of the jet at standoff S to that at $S = 0$ is assumed to be $(1 + \beta S)^2$ from [1]. Other models, due to Pugh [3, 6], assume that the ratio of the cross-sectional area of the jet at standoff S to that at $S = 0$ is $1 + \beta S^2$ instead of $(1 + \beta S)^2$. In either model, the constants α and β must be determined experimentally.

Pack and Evans [5] also noted the importance of target material strength on jet penetration. To account for strength, they proposed correcting equation (2) by a semi-empirical factor

$$P = \left(\frac{\rho_j}{\rho_t}\right)^{1/2} L\left(1 - \frac{\alpha Y}{\rho_j V^2}\right). \tag{11}$$

They showed that for steel, the correction term $\alpha Y / \rho_j V^2$ is as great as 0.3; that is, the effect of strength is to reduce penetration by as much as 30%.

For the penetration of ductile targets, such as lead, by a shaped-charge jet, Pack and Evans [5] modified equation (11) by adding a secondary penetration term equal to the radius of the hole made by the jet.

Significant progress was made in 1955, when Eichelberger [7] conducted penetration vs time measurements. He verified that the hydrodynamic formula, equation (1), is very accurate for early times and short standoffs where the jet has a high velocity and is not yet broken. He found that when the jet is broken, λ in equation (4) should actually be less than 1 if ρ_j is taken as the original density of the liner. Furthermore, at low jet speeds, the strengths of the jet and target are important. Eichelberger proposed the formula

$$\lambda \rho_j (V - U)^2 = \rho_t U^2 + 2\sigma, \tag{12}$$

where $\sigma = \sigma_t - \sigma_j$, in which σ_t and σ_j are the 'resistance to plastic deformation' for the target and jet, respectively. These strength terms are taken as one to three times the static uniaxial yield stress, with the factor attributed to strain-rate effects and to the state of non-uniaxial stress at the yield site in the target.

Beyond this point, the quasi-steady hydrodynamic theory has evolved along two lines: the shaped-charge jet with variable velocity, and the kinetic-energy rod with uniform initial velocity. For stretching jets, work has been directed toward analytical solutions and quantifying the degradation in penetration beyond the point of jet breakup. For rods of uniform velocity, models treating the deceleration and deformation (shortening) of the penetrator have been developed; these models are applicable to broken jets or short length-to-diameter ratio rods.

Variable velocity jets

For a jet of non-uniform velocity distribution, such as that produced by a shaped charge, the jet length is not constant but increases with time. In this case, equation (2) is not directly applicable.

As a first step, Abrahamson and Goodier [9] derived explicit formulae for the penetration of continuous straight jets of non-uniform velocity. They concluded that if strength is neglected, addition of a constant velocity over the entire jet actually decreases penetration, since the jet has less time to stretch before penetrating. If, however, the rear of the jet is too slow to overcome the strength of the target, addition of a uniform velocity may increase penetration. They derived a formula for the penetration of an idealized jet, which serves as a theoretical maximum. In their analysis, they took the jet length as known at a given distance from the target, but did not consider the relationship between jet length and distance from the charge; this makes their results less useful for practical purposes.

Allison and Vitali [10] further extended the theory to account for jet segmentation, with the following assumptions and conclusions.

(a) *Existence of a virtual origin.* It is known that the velocity of each jet particle remains nearly constant. If, in addition, the spatial distribution of velocity is linear, as for most jets from constant-thickness conical liners, then a 'virtual origin', or point source, of the entire jet can be located, as first proposed by Allison and Bryan [11].

(b) *Negligible strength.* The strengths of the jet and target materials were neglected by Allison and Vitali [10]. So, to characterize the termination of the penetration by the slow-moving rear of the jet, a minimum jet velocity for penetration, V_{min}, is defined. This V_{min}, and the penetration process at low velocity, must depend on the strengths of the jet and target. This is an artificial method to terminate the penetration.

(c) *Negligible compressibility.* They also studied the effect of compressibility on penetration from equation-of-state data and the compressible-flow Bernoulli's equation. They concluded that firstly there is no effect for like jet and target materials and secondly, for dissimilar materials, the effect is small, provided the compressibilities do not differ greatly (e.g. only 1% difference in penetration velocity between the compressible and incompressible flow equations for a copper jet against a titanium target at shaped-charge velocities). Harlow and Pracht [12] confirmed this in two-dimensional code simulations of iron and aluminum jets impacting similar targets. (It will be shown below that compressibility is indeed negligible for a metal jet on a metal target; for a metal jet on a low-sound-speed target, such as Plexiglas, compressibility is not insignificant.)

Before jet breakup, penetration P as a function of time t was derived by Allison and Vitali as

$$P(t) = V_0 t (t_0/t)^{\gamma/(1+\gamma)} - t_0 V_0, \tag{13}$$

where $\gamma = (\rho_t/\rho_j)^{1/2}$ and t_0 is the time of arrival at the target of the jet tip, which has velocity V_0.

(d) *Simultaneous breakup.* In Ref. [10], the entire jet is assumed to break simultaneously. This assumption has also been used by other investigators [13–17]. In general, for conventional shaped charges, where the jet particulates or breaks up from tip to tail, the simultaneous jet breakup assumption is, at best, a first-order approximation. Usually, as verified by the studies of Simon *et al.* [13–17], this assumption is satisfactory for conventional warheads.

In reality, there exists a distribution of jet particulation from tip to tail where several microseconds are required before particulation is complete. For unconventional warheads, where the breakup does not proceed from tip to tail, this assumption (of a simultaneous, constant, breakup time) is invalid.

(e) *Each broken-jet segment penetrates as a continuous jet.* The basic principles involved in Eichelberger's hydrodynamic penetration theory are Bernoulli's equation and the continuity equation,

$$\frac{\mathrm{d}P}{U} = -\frac{\mathrm{d}\xi}{V-U}, \tag{14}$$

where $\mathrm{d}\xi$ is the incremental length of the jet. Allison and Vitali, in calculating the penetration of a segmented jet, assumed that equations (1) and (14) are applicable for short separated jet segments as well. This assumption is questionable, because the penetration of finite segments is affected more by unsteady effects and is often less than that calculated from steady formulae. Under this assumption, once the jet breaks, penetration remains constant with further increase in standoff. In reality, penetration decreases with standoff after the jet is broken. Experiments by Chou *et al.* [18, 19] indicated that the penetration of two segments with an intervening gap is less than that of two segments with no gap. Two-dimensional computer-code calculations by Harlow and Pracht [12] also demonstrated that, during the initial transient period, penetration is less than in the steady-state case.

The principles proposed by Allison and Vitali are still used today as the basis for penetration calculations. Dipersio and Simon [14] presented explicit formulae based on Allison and Vitali's theory, for three cases: (a) penetration before jet breakup ($T \leqslant t_b$), (b) jet breaks during penetration ($t_0 < t_b \leqslant T$) and (c) jet breaks before reaching the target ($t_b \leqslant t_0 \leqslant T$), where T is the time at the end of penetration, t_b the time of jet breakup and t_0 the time when the tip reaches the target. For case (a), the total penetration depth P is

$$P = S[(V_0/V_{min})^{1/\gamma} - 1], \tag{15}$$

where S here is the distance from the virtual origin to the target, or the effective standoff distance. In this case S is bounded by

$$0 \leqslant S < V_{\min} t_{\mathrm{b}} \left(\frac{V_{\min}}{V_0} \right)^{1/\gamma}$$

and

$$U_{\min} = \frac{V_{\min}}{1+\gamma}.$$

For case (b), the penetration is

$$P = \frac{(1+\gamma)(V_0 t_{\mathrm{b}})^{1/(1+\gamma)} S^{\gamma/(1+\gamma)} - V_{\min} t_{\mathrm{b}}}{\gamma} - S, \tag{16}$$

where S is bounded by

$$V_{\min} t_{\mathrm{b}} \left(\frac{V_{\min}}{V_0} \right)^{1/\gamma} < S < V_0 t_{\mathrm{b}}.$$

Finally, for case (c), the penetration is

$$P = \frac{(V_0 - V_{\min}) t_{\mathrm{b}}}{\gamma} \tag{17}$$

for standoffs in the range given by

$$V_0 t_{\mathrm{b}} < S < \infty.$$

Recall that $\gamma = \sqrt{\rho_{\mathrm{T}}/\rho_{\mathrm{j}}}$.

The formulae given above are the results of the so-called DSM (DiPersio, Simon and Merendino) theory [14]. Other works related to studies of this type are given in Refs [13–17, 20–26].

The above equation may be re-arranged to yield the velocity V_{p} of that point in the jet that is currently penetrating at a depth P in the target. For example, equation (15) becomes

$$V_{\mathrm{p}} = V_0 \left[\frac{S}{P+S} \right]^{\gamma}.$$

This is also, of course, the emergent velocity of a continuous jet after penetrating a target of finite thickness P.

Based on equations (15–17), DiPersio and Simon [14] also compared their calculated penetration depth with experimental data. In general, good agreement was obtained at short standoffs, up to about three charge diameters. At larger standoffs, the formulae give higher than measured values. They attributed the declining performance of actual jets mainly to asymmetric wavering of the jet.

In 1965, DiPersio, Simon and Merendino [17] conducted an extensive experimental program to determine the causes of decreased penetration at long standoff. They reached the following conclusions:

(a) Jets from precision charges travel in very straight lines; jet particles show no appreciable tumbling, deceleration or mass ablation due to air friction. For conical liners, the jet-velocity distribution is nearly linear, and the assumption of a virtual origin is valid.

(b) The minimum jet velocity for penetration is not constant for a given jet or target, but increases with standoff.

Since $V_{\min}$ is not a constant, they proposed a new criterion for terminating penetration based on a minimum penetration velocity $U_{\min}$. From test data they noticed that the penetration velocity U at the time penetration stops was constant for different standoffs. The penetration velocity of a broken jet was obtained, in essence, by drawing a smooth curve through the penetration history. The slope of this curve at the cessation of penetration was taken to be a constant, $U_{\min}$, regardless of standoff. For the standard charge they used, $U_{\min}$ was about 1.0 km s^{-1}.

Next, DiPersio and Simon modified the penetration formulae in all three regimes by replacing the $V_{\min}$ criterion with a $U_{\min}$ criterion. The new formulae yield penetrations that decrease with standoff, in better agreement with experimental data [17].

Equations (15–17) were taken to be valid except those equations that contain the term $V_{\min}$. Equations for the jet velocity and the penetration velocity were derived. The equations for the total penetration, using $U_{\min}$ as a jet cut-off criterion instead of $V_{\min}$, are given below. For case (a),

$$P = S\left[\left(\frac{V_0}{(1+\gamma)U_{\min}}\right)^{1/\gamma} - 1\right], \tag{18}$$

where S is bounded by

$$0 \leqslant S < (1+\gamma)U_{\min}t_b\left[\frac{(1+\gamma)U_{\min}}{V_0}\right]^{1/\gamma}.$$

For case (b), the penetration is now

$$P = \frac{(1+\gamma)(V_0t_b)^{1/(1+\gamma)}S^{1/(1+\gamma)} - \sqrt{(1+\gamma)U_{\min}t_b(V_0t_b)^{1/(1+\gamma)}S^{\gamma/(1+\gamma)}}}{\gamma} - S, \tag{19}$$

where S ranges from

$$(1+\gamma)U_{\min}t_b\left[\frac{(1+\gamma)U_{\min}}{V_0}\right]^{1/\gamma} < S < V_0t_b.$$

For case (c), when the jet particulates before penetration begins,

$$P = \frac{V_0t_b - \sqrt{U_{\min}t_b(V_0t_b + \gamma S)}}{\gamma}, \tag{20}$$

where S lies in the interval

$$V_0t_b < S \leqslant \frac{V_0t_b}{\gamma}\left(\frac{V_0 - U_{\min}}{U_{\min}}\right)$$

and $P = 0$ when S equals its upper bound.

For the $U_{\min}$ criterion, equations (18–20) are used in lieu of equations (15–17), respectively. The total length of jet which contributes to the penetration process may be obtained by multiplying the appropriate value of P [from equation (18), (19) or (20)] by γ.

DiPersio and Simon subsequently conducted many informative experiments. In 1966 [15], they reported a study on 'residual penetration'—penetration by a jet into a main target after perforating a series of skirting plates. In 1968 [16], they studied the effect of jet breakup on penetration (the earlier the breakup, the less the penetration), and discussed the effect of jet rotation. In Refs [20, 23, 26], they verified experimentally that penetration decreases as target strength, or hardness, increases. Merendino and Vitali made the same observation [21].

In Ref. [22], Simon and DiPersio, using flash radiography and other techniques, revealed that the rear portion of the jet that does not contribute to penetration actually piles up at the bottom of the hole. They also mentioned a 'valve action', whereby the rear of the jet is trapped by the small hole created by the front of the jet. References [17, 20, 22–26] present several comparisons of the DSM theory with experimental data.

Note that in all these studies the basic hydrodynamic equation (1) was used to describe the penetration process, while efforts were made to determine the termination of penetration, $V_{\min}$ or $U_{\min}$, by empirical means.

Eichelberger's formula, equation (12), which contains the material strength term, was not used at all. Thus, the material is described only by an empirical constant and its density.

The penetration criteria based on the minimum velocities $V_{\min}$ and $U_{\min}$ provide useful practical formulae, but do not directly address the physical causes of the decrease in jet

penetration with standoff. These phenomena, which include jet segmentation, wavering and tumbling of jet particles, have been the focus of several recent studies. Note that since U is the penetration velocity and by definition $U = \dot{P}$, so U_{min} (the minimum penetration velocity) is zero when the penetration ceases, or when the penetration–time curve asymptotes.

It is generally recognized that three-dimensional effects (or two-dimensional effects if the target is impacted at normal obliquity) are the true mechanisms involved in jet cutoff or penetration termination. A U_{min} or V_{min} cutoff criterion is simply a device to allow the one-dimensional models to be effective. This is not meant as a criticism of the DSM theory alone, since all analytical models suffer this limitation. Basically, the DSM limitation is in the *a priori* determination of U_{min}, which is often not a constant, but varies strongly with standoff and charge diameter for a given jet–target configuration. This is documented in the CUMIN report [27] where Majerus and Scott provided several plots of the U_{min} variation. Unfortunately, this variation of U_{min} with standoff and charge diameter is highly erratic and cannot be readily modelled or curve fit. Nonetheless, Ref. [27] is a useful aid in the application of the DSM theory.

Jet wavering, jet tumbling, jet drift and crossing (or transverse) velocity effects (where the target moves as the jet penetrates) have been analyzed by several authors. Notably, these analyses are found in Majerus *et al.* [28] and Segletes [29] on the effects of transverse velocity, Segletes [30] on the effects of jet drift velocity and Held [31] and Golesworthy [32] on the effects of transverse velocity.

Particulated jets

Carleone *et al.* [33], in an augmented version of the one-dimensional jet-formation code DESC, developed a theory for predicting the breakup of shaped-charge jets and introduced an approximate method for determining the decrease in penetration with standoff. First, the breakup time of each portion of the jet is calculated or measured. If a given segment of jet reaches the target before its computed breakup time, its penetration is calculated from Eichelberger's equation (4), for a continuous jet. If the segment of jet has broken, however, its actual penetration dP' is deduced from the continuous-jet penetration dP by the formula

$$dP' = dP\left(1 - \frac{g}{g_0}\right), \tag{21}$$

where g is the gap distance between jet particles, non-dimensionalized with respect to the increment of jet length, and g_0 is an empirical constant. According to this formula, penetration is degraded as the particles move farther apart, so that after breakup, penetration decreases (as expected) with standoff. Comparisons with experimental data show good agreement when $g_0 = 6.5$ for precision shaped charges and 4–6 for non-precision or small charges. An advantage of this simple theory is that only one empirical constant need be specified.

A more sophisticated approach was taken by Smith [34], who applied the Monte Carlo technique to the effects of tumbling, dispersion (or wavering) and breakup, which are considered as stochastic processes. The values of the parameters governing these processes are assumed to follow prescribed probability distributions. Then, random values consistent with these distributions are chosen for the parameters of each jet particle. Finally, jet penetration is determined by applying Tate's method for rod penetrators [35] (discussed later) to each particle. With proper selection of the statistical parameters (mean, standard deviation) describing the distributions of tumbling rate, dispersion angle and breakup time, excellent agreement with measured penetrations can be achieved. The chief shortcoming of this approach is the difficulty in determining, *a priori*, proper values for all of these parameters. Nevertheless, this method is useful for interpolating and extrapolating penetration data; once the parameters have been calibrated by experimental data, penetrations at other standoffs or against other targets can be estimated with some confidence. Improvements to this model [34] are possible by coupling the Monte Carlo

technique with a model more suitable to shaped-charge penetration than Tate's rod model [35].

Zaid [36] formulated a penetration–perforation model based on the conservation of mass and momentum. Zaid considered shear stress terms and modelled a non-deforming cylindrical penetrator.

Majerus and Walters [37–43] developed a penetration model based on the conservation of mass and momentum using an integral approach and a control-volume concept. They divided the penetration process into two regions, the undeformed portion of the penetrator and the interaction region of deforming target and penetrator materials at the bottom of the crater. Global equations of motion are derived for each region in terms of normal stresses and shear stresses, the latter using a Newtonian fluid approximation. The resulting system of ordinary differential equations is solved by numerical integration. With proper selection of values for target strength and viscosity, good agreement with measured penetration can be achieved. The dynamic viscosity values are obtained from the U.S. or U.S.S.R. experimental data. See Refs [36–42], for example. The strength term represents a dynamic value analogous to that used in equations (11) and (12), for example.

Walters and Majerus used an approximation of broken jets involving two steps. First, the broken jet is replaced by a continuous jet of equal length, of density the same as the average of the broken jet, as suggested by Allison and Vitali [10]. Then the continuous jet is shortened to the sum of the lengths of the particles in the original jet. This method yields satisfactory results but gives no insight into the mechanism of penetration by broken jets.

The model defines the termination of penetration to occur when U, the penetration velocity, reaches zero. This can happen after the jet length (which is also calculated) is consumed, thereby providing a measure of the secondary penetration or afterflow. The model is also capable of analyzing layered, multi-material targets including air gaps [41].

The conservation of momentum yields

$$\frac{\mathrm{d}}{\mathrm{d}t}(MU) = \pi r_j^2(\sigma_j - \sigma_T) + \pi r_j^2 \rho_0 (V_I - U) - \pi r_j^2 \rho_{T_0} U^2 - 2\pi \dot{H}_0 \mu U \qquad (22)$$

for a continuous jet. In this equation M is the mass of the jet, U is the penetration velocity, r_j is the jet radius, σ_j and σ_T are the dynamic strength values of the jet and target, respectively, ρ_0 and ρ_{T_0} are the jet and target densities, respectively, H_0 is the height of the interaction region between the penetrator and the target and V_I is the velocity at the top of the interaction region. References [37–43], especially [41], present the derivation of equation (22) and provide analogous equations for particulated jets. Expressions for V_I, H_0, r_j and the jet length are also given for continuous and particulated jets. The jet length, jet radius and jet density determine the jet mass M. References [37–43] present several penetration depth and penetration time predictions and comparisons with experimental data. References [37–40] extend the model to include penetration by long or short rods.

One interesting application of this model was the accurate prediction of the data presented in Ref. [3]. In that work, a series of 1 in. plates of lead were stacked and a single 1 in. RHA (rolled homogeneous armor) plate was inserted in the stack at various depths, e.g. first as the top plate, then as the second plate, etc. The test objective was to plot penetration into the stack as a function of the position of the hard (RHA) plate from the top of the stack. For penetration by a shaped-charge jet, there exists an optimum position of the hard plate from the top to minimize the penetration. The experiment was also conducted using mild steel plates instead of lead. The Walters–Majerus model [43] successfully predicted the optimum location of the RHA plate for either case given in Ref. [3] and for a new experimental test using an RHA plate in an aluminum stack. In addition, this effect was found to be standoff-dependent; see Fig. 4, for example, where an RHA plate in a lead stack was analyzed. This study was significant in that many models experience difficulty in providing accurate penetration depth and penetration time predictions into multi-material layered targets since any material parameters or semi-empirical constants in use must change during the penetration process.

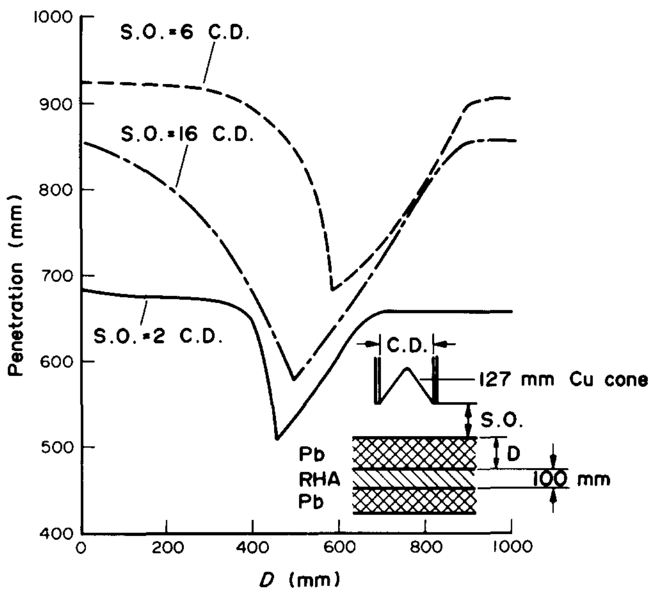

FIG. 4. Predicted penetration vs a layered target, from Walters *et al.* [43].

Most other models in use are based on an extension or duplication of those described in this section. For example, a simple analytical model based on the concepts given earlier was developed by Szendrei [44]. Other models that contain original concepts are due to Evans and Ubbelohde [45, 46], Luttwak *et al.* [47], Andersson *et al.* [48], Sagomonyan [49] and Murphy [50].

A frequently used model for shaped-charge jet penetration follows from Alekseevskii [51], Sanasaryan [52] and Sagomonyan [53–55]. The simple penetration model is based on a modified Bernoulli equation,

$$H_D + k_T \rho_T U^2 = \sigma_{SD} + k_j \rho_j (V - U)^2, \tag{23}$$

using the notation introduced earlier, and where H_D is the dynamic hardness of the target, taken as the Vickers hardness. The terms k_T and k_j are the body shape factors of the target and jet, respectively, which depend on the flow geometry and the effect of internal forces; they are difficult to determine—Alekseevskii [51] takes $k_T = k_j = 1/2$. Finally, σ_{SD} is the part of the stress state of the deforming penetrator determined by the internal forces, and is called the dynamic yield point [51]. The cutoff velocity, or velocity below which the jet will cease to penetrate, akin to the V_{min} of the DSM theory discussed earlier, is

$$V_{min} = \sqrt{\frac{H_D - \sigma_{SD}}{k_j \rho_j}}. \tag{24}$$

Equation (24) follows from equation (23) for $U = 0$. Since $U = \dot{P}$, determination of U implies P by numerical integration.

Compressible models

As discussed earlier, Allison and Vitali [10] and Harlow and Pracht [12] indicated that the effect of compressibility on penetration of metal jets into metal targets is slight. However, Haugstad and Dullum [56, 57] showed that for non-metallic targets, compressibility effects may be significant. Furthermore, if the jet velocity is sufficiently high for shocks to occur, the penetration can be much less than that predicted by the incompressible theory (20% reduction for a copper jet against plexiglas at 10 km s^{-1}).

The form of the Bernoulli equation presented earlier neglects compressibility, consideration of which requires an additional term (the flow work) that depends on the compressibilities of the jet and target materials. If the compressibilities are similar (as for a copper jet impacting a steel target), this term is negligible. If the target is appreciably more

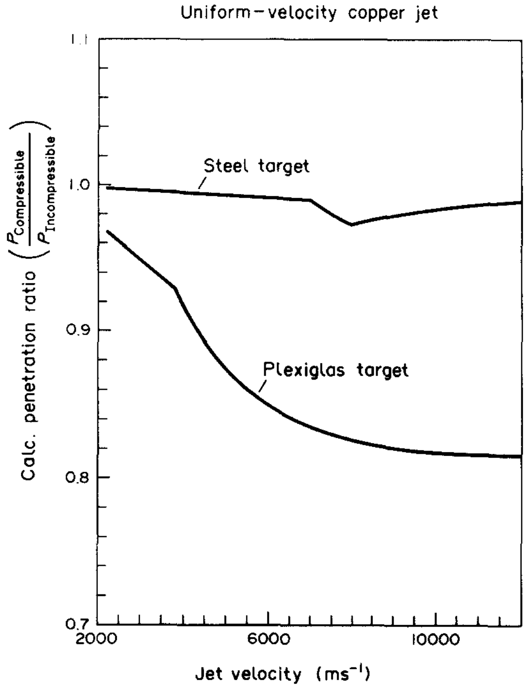

FIG. 5. Effect of compressibility on penetration by a uniform-velocity copper jet [58].

compressible than the jet (as for a copper jet against a plexiglass target), the effect of this term is to significantly reduce penetration as compared to incompressible flow theory, as shown in Fig. 5.

Flis and Chou [58] extended the compressible theory to include more general equations of state (including Mie-Gruneisen and Tillotson), and reconfirmed the conclusions of previous researchers. They also applied the compressible model to a stretching jet using the virtual-origin assumption, and showed that the penetration of such a jet can theoretically be as much as 50% less than predicted by the incompressible theory. This greater degradation in penetration for a stretching jet is explained by observing that, when the front of the jet penetrates less, the rear portion has less distance to stretch, and therefore also penetrates less.

Experimental evidence of the importance of compressibility has not been convincing. Experiments by White et al. [59, 60] of non-precision shaped charges against plexiglas, aluminum, steel and several liquids as target materials showed no correlation of target penetration resistance with compressibility.

Chick et al. [61] applied the compressible theory to a jet with non-linear velocity distribution, for which a virtual origin was not assumed. For such a jet projected by a small copper-lined conical charge into a plexiglas target, a difference in penetration rate of only about 4% is predicted by the compressible and incompressible theories, but they claimed that their experimental results were in better agreement with the compressible theory. Coincidentally, they point out that, for their jet, the error involved in neglecting compressibility is comparable to that involved in assuming a single virtual origin for the entire jet.

Woidneck [62] fired copper rod projectiles into water, glycerol and methanol at velocities of 2500 and 5000 m s^{-1}. Even at the higher velocity, the effect of compressibility makes a difference of only 3.3% (for water) in the early-time penetration rate, which he did not discern in his experiments.

The virtual origin concept

The virtual origin concept is used in penetration calculations to determine the effective standoff distance and to allow an accurate prediction of short standoff penetration. Most of the penetration models assume that the jet velocity is linearly distributed in space and rely on

the virtual origin approach first used by Allison and Vitali [10] to integrate the penetration over the length of the jet. Recently, Chou *et al.* [63] examined the accuracy of the virtual origin approximation, concluding that for charges with simple conical or hemispherical liners, the maximum error involved is less than 0.2 charge diameters and is constant with standoff. However, Foster [64], using a mass-summation technique to analyze jet radiographs before breakup, has shown a significant non-linearity in the velocity distribution of a biconic shaped charge.

Uniform velocity rods

Uniform velocity rod models are often used in shaped-charge penetration and SFF or EFP penetration studies. Note that there is some analogy between penetration by rods and shaped-charge jets in that pure rod models are sometimes adapted for shaped charge penetration studies, e.g. Smith [34], Alekseevskii [51] and Sanasaryan [53]. Some noteworthy differences are in the target strength effects which are usually more predominant for rod-like projectiles which experience typically lower impact velocities than shaped-charge jets. Thus, penetration by a shaped-charge jet represents a closer approximation to purely hydrodynamic flow than rod projectiles. For a shaped-charge jet, the jet velocity can be established, since the velocity gradient of the jet from tip to tail is approximately linear. However, for rod-like projectiles, which deform and erode and do not penetrate at a constant velocity, the rod velocity during penetration (as well as the penetration velocity) is unknown. On the other hand, for shaped-charge jet penetration studies, one must consider the eventual breakup of the jet and analyze penetration of segmented jet particles.

Allen and Rogers [65] conducted a series of experiments with rods of various materials impacting aluminum targets. Comparing their data with Eichelberger's formula, equation (12), they concluded that the net strength $\sigma = \sigma_t - \sigma_p$ is nearly independent of penetrator material, or that σ_p is negligible compared to σ_t. Further, they postulated that the target strength is strain-rate dependent and expressed σ_t as a function of the penetration velocity U. In addition, they observed 'secondary penetration' in high-velocity impacts of dense (gold) rods against light (aluminum) targets. In this case, at the end of the usual penetration process, penetrator material that has been deflected by the crater bottom still has a net velocity into the target and can thus cause additional penetration.

Christman and Gehring [66] developed a model by considering the effects of the primary and secondary phases of penetration. For a velocity range of 2.0–6.7 km s^{-1}, they report good agreement with experimental data. The dimensionless penetration into semi-infinite metal targets is expressed as

$$\frac{P}{L} = \left(1 - \frac{D}{L}\right)\left(\frac{\rho_p}{\rho_t}\right)^{1/2} + 2.42\frac{D}{L}\left(\frac{\rho_p}{\rho_t}\right)^{2/3}\left(\frac{\rho_t V^2}{B_{max}}\right)^{1/3}. \tag{25}$$

The first term represents the primary (or hydrodynamic) phase of penetration. The effective length of the penetrator for this phase is reduced by one rod diameter. This remaining diameter of length is assumed to contribute to the secondary phase of penetration, as represented by the remaining empirical term. The terms are self-explanatory, except perhaps B_{max}, the Brinell hardness of the target. This model allows the final penetration to be greater than that predicted by the one-dimensional, hydrodynamic theory.

Doyle and Buchholz [67] used a modified form of the Christman–Gehring equation (25) to predict the penetration of mass focused slugs (or EFPs) at long standoff distances. Their equation was

$$\frac{P}{L} = \left(1 - \frac{D}{L}\right)\left(\frac{\rho_p}{\rho_t}\right)^{1/2} + \frac{0.13}{L}\left(\frac{\rho_p}{\rho_t}\right)^{1/3}\left(\frac{E_1}{B_{max}}\right)^{1/3}, \tag{26}$$

where

P = target penetration depth (inches),
L = length of projectile (inches),
D = diameter of projectile (inches),

ρ_p = density of projectile,
ρ_t = density of target,
E_1 = energy in last caliber (last part) of the projectile (joules),
B_{max} = target hardness beneath the penetrating projectile (kg mm^{-2}).

From Ref. [67], Doyle and Buchholz state that equation (26) essentially assumes that the first part of the slug (all except the last caliber) performs like a shaped-charge jet. The last part (last caliber) performs like a ballistic projectile. Thus, total penetration in metallic targets can be represented by this two-part equation that separates the contributions from primary and secondary penetration phases. Primary penetration is a function of projectile length and density and target density. Secondary penetration is a function of projectile density and kinetic energy and target density and strength.

A major contribution to the one-dimensional theory of rod penetration was made by Tate [35, 68–73], who accounted for the deceleration and shortening of the rod during penetration. (A similar model was developed independently by Alekseevskii [52].) Equation (12), the Bernoulli equation with strength, is used with the equation of motion of the undeformed part of the rod

$$\rho_p L \frac{dV}{dt} = \sigma_p \tag{27}$$

and the kinematic relation $dL/dt = V - U$, where L is the current length of the rod. Tate presented several explicit solutions to this system of equations for special cases of density and material strength; the general case may be solved by numerical integration. Tate recommended the value of σ_p as the Hugoniot elastic limit of the projectile material and σ_1 as 3.5 times the Hugoniot elastic limit of the target material.

Tate considered two classes of impacts, $\sigma_p > \sigma_t$ and $\sigma_p < \sigma_t$. In the former case (hard penetrator, soft target), the penetration process passes through two stages: at a sufficiently high impact velocity, the penetrator and target first both flow hydrodynamically; later, after the penetrator has decelerated, it ceases to flow and penetrates as a rigid body. When a soft penetrator impacts a hard target (the case of most interest), both materials initially behave hydrodynamically; then, after the penetrator decelerates below a critical velocity, the target ceases to flow so that penetration stops, while the penetrator continues to deform. For both cases, if the impact velocity does not exceed a critical velocity calculated from equation (12), the initial stage of purely hydrodynamic behavior is absent. These phenomena are summarized in the phase diagram, Fig. 6, introduced by Chou and Flis [74].

Chou and Flis suggested a different set of values for σ_p and σ_t. They reasoned that, since the deforming part of the penetrator is in a state of uniaxial stress, σ_p should be chosen as the uniaxial yield stress rather than the Hugoniot elastic limit (the strength under a condition of uniaxial strain). Then, by comparing with experiments and hydrocode calculation, they showed that taking the target resistance σ_t as 2.5 times the Hugoniot elastic limit gave the best agreement. In addition, in a computer code for integrating Tate's equations [74], they included an approximate method for computing the secondary penetration observed by Allen and Rogers, and also by Tate.

An Integral Theory of impact has been developed by Donaldson and Contiliano and others [75, 76]. This theory was extended to include a rod penetrator model applicable to a wide range of impact velocities and materials. Good correlations with experimental data have been reported. The penetrator is modelled as a head, from which material can erode, and a rigid shaft that is decelerated by interface stresses at the head. The target material is characterized by two properties: E_{*p}, the energy absorbed during plastic deformation, and E_{*e}, that absorbed by elastic deformation. Simple formulae have been derived to determine these constants from laboratory tests. The determination of these constants for a variety of materials has identified certain hard, brittle, non-metallic materials as effective armor materials.

In Fig. 7, three calculations are compared based on Tate's deceleration model (using the RODPEN code [74]), Donaldson's integral theory of impact and Christian and Gehring's

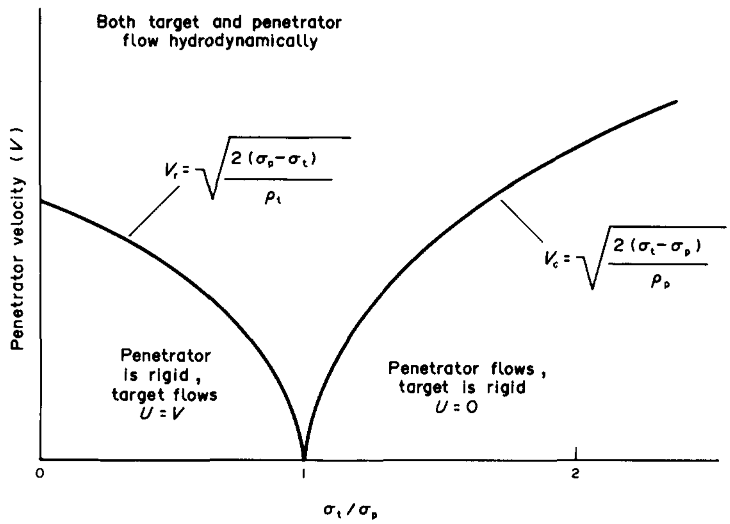

FIG. 6. Phase diagram of rod penetration according to one-dimensional theory.

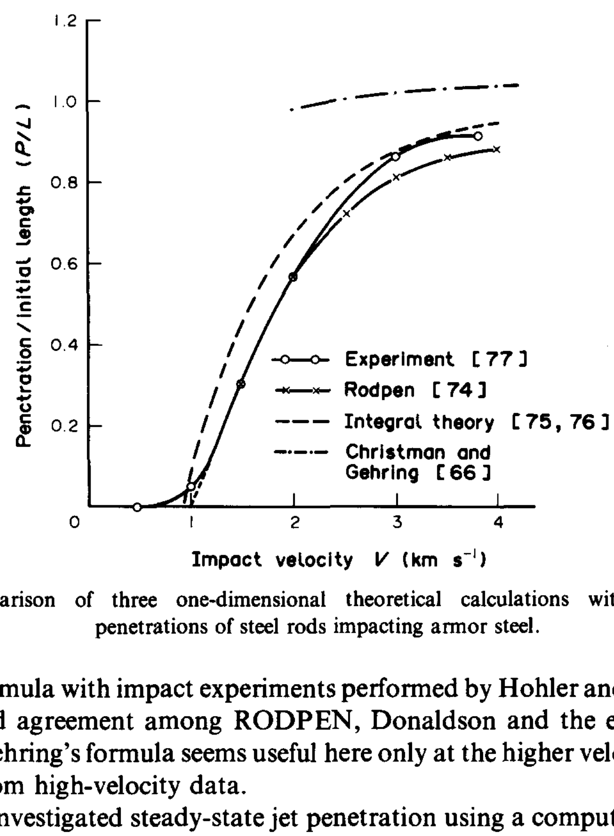

FIG. 7. Comparison of three one-dimensional theoretical calculations with experimental penetrations of steel rods impacting armor steel.

semi-empirical formula with impact experiments performed by Hohler and Stilp [77]. These results show good agreement among RODPEN, Donaldson and the experiments, while Christman and Gehring's formula seems useful here only at the higher velocities, and indeed was developed from high-velocity data.

Matuska [78] investigated steady-state jet penetration using a computational approach. From simulations with the two-dimensional Eulerian hydrocode HULL, he determined the values of the parameters in a modified form of Bernoulli's equation,

$$\frac{\gamma}{2}\rho_j(V-U)^2 + \beta\sigma_j = \frac{\rho_t U^2}{2} + \alpha\sigma_t. \tag{28}$$

The values determined for the parameters are:

$\alpha = 1$

$\beta = 0.3$

$\gamma = 0.47 + 0.028\rho_j + 0.00086\rho_j^2 + 0.072 \ln V.$

The deviation of γ from its theoretical value of unity was attributed to the target's resistance

to radial flow. This deduction was based on results of simulations of two impinging jets of equal radius, for which γ had a value very close to 1.

This model was extended to rod penetrators by substituting the above equation for the Bernoulli equation in Tate's model. The steady-state portion of penetration is calculated by numerically integrating the resulting equations. Steady-state penetration is considered to cease when the rod has eroded to a length equal to its diameter (as suggested by [66]) or when the penetration velocity has dropped to a prescribed value.

Other rod models and data are discussed by Walters and Majerus [37], Belyayev *et al.* [79], Weihrauch [80] (an excellent experimental study), Clark [81] and Dehn [82], who discusses the history of rod penetration, presents a survey of rod penetration models and develops new rod penetration concepts based on estimated or semi-empirically determined parameters. Allen *et al.* [83] introduce a drag coefficient concept and present a model for a non-eroding bullet penetrating sand.

Excellent surveys of penetration by rods are given by Wright [84], Backman and Goldsmith [85], Dehn [82], and in the books by Goldsmith [86] and Johnson [87]. Studies involving rod penetration, experimental data and hydrocode simulation are given by Jonas and Zukas [88, 89] and Zukas [90]. Zukas summarizes much of the penetration and hydrocode simulation methods in his book [91].

As a final note, Chou and Flis [92] recently published, in part, some of the material presented earlier, such as one-dimensional hydrodynamic theory, two-dimensional theory, variable-velocity jets, compressible penetration models, virtual origin concepts and uniform-velocity rod penetration. The current report elaborates upon and expands the abbreviated discussion of [92].

Also, Dehn [93] recently published a generalized equation of motion for penetration. In various specialized forms, this equation is used to calculate penetration by rods, jets or fragments. The generalized equation of motion describes the target force resisting penetration as a second-order polynomial in the penetration speed. The force and coefficients of the penetrator speed must be determined for each case. This equation was also presented by Johnson [87] and Allen *et al.* [83] and is a generalized form of the Robins–Euler equation. Dehn [93] also provides a comprehensive overview and survey of jet and rod penetration models.

CONCLUSIONS

Several analytical models used to calculate the penetration of a shaped-charge jet were presented. These models range from those of historical value, which provided the foundation for later models, to models currently in use. An overview of some of the available models was presented. No comparison was made regarding the relative accuracy of any of these models since they all involve either dynamic material properties of unknown value or semi-empirical parameters that must be determined for the given penetrator–target configuration. Thus, the choice of a penetration model depends on the input available to the user and his experience with a particular model.

An extensive reference list is provided to guide others in choosing a model or in developing a new model.

REFERENCES

1. G. BIRKHOFF, D. MACDOUGALL, E. PUGH and G. TAYLOR, Explosives with lined cavities. *J. appl. Phys.* **19**, 563–582 (1948).
2. R. HILL, N. MOTT and D. PACK, A.R.D. Theoretical Research Report No. 2/44 (January 1944) and 13/44 (1944).
3. CARNEGIE INSTITUTE OF TECHNOLOGY, Protection against shaped charges. NRDC Report No. A-384 and OSRD Report No. 6384 (1946).
4. W. M. EVANS, The hollow charge effect. *Bull. Inst. Min. Metall.* **520**, 9–25 (1950).
5. D. C. PACK and W. M. EVANS, Penetration by high-velocity ('Munroe') jets: I. *Proc. Phys. Soc. (Lond.)* **B64**, 298 (1951).

6. E. M. PUGH, A theory of target penetration of jets. National Defense Research Committee Armor and Ordnance. Report No. A-274 (OSRD No. 3752) Division 2 (1944).
7. R. J. EICHELBERGER, Experimental test of the theory of penetration by metallic jets. *J. appl. Phys.* **27**, 63–68 (1956).
8. G. BIRKHOFF, Hollow charge anti-tank (HEAT) projectiles. Ballistic Research Laboratories Report No. 623 (1947).
9. G. R. ABRAHAMSON and J. N. GOODIER, Penetration by shaped-charge jets of nonuniform velocity. *J. appl. Phys.* **34**, 195–199 (1963).
10. F. E. ALLISON and R. VITALI, A new method of computing penetration variables for shaped-charge jets. Ballistic Research Laboratory Report No. 1184 (1963).
11. F. E. ALLISON and G. M. BRYAN, Cratering by a train of hypervelocity fragments. *Proc. 2nd Hypervelocity Impact Effects Symp.*, Vol. 1, p. 81 (1957).
12. F. H. HARLOW and W. E. PRACHT, Formation and penetration of high-speed collapse jets. *Phys. Fluids* **9**, 10 (1966).
13. J. SIMON, R. DIPERSIO and A. B. MERENDINO, Penetration capability and effectiveness of a precision shaped-charge warhead. Ballistic Research Laboratory Memorandum Report No. 1636 (1965).
14. R. DIPERSIO and J. SIMON, The penetration–standoff relation for idealized shaped charge jets. Ballistic Research Laboratory Memorandum Report 1542 (1964).
15. R. DIPERSIO and J. SIMON, Theory of residual penetration by ideal shaped charge jets. Ballistic Research Laboratory Report No. 1313 (1966).
16. R. DIPERSIO and J. SIMON, The effect of jet breakup time on the penetration performance of shaped charges. Ballistic Research Laboratory Memorandum Report No. 1897 (1968).
17. R. DIPERSIO, J. SIMON and A. B. MERENDINO, Penetration of shaped-charge jets into metallic targets. Ballistic Research Laboratory Memorandum Report No. 1296 (1965).
18. P. C. CHOU, M. MINNICH and L. GAUSE, Experimental study of multiple interior impacts. Ballistic Research Laboratory Contract Report No. 199 (1975).
19. P. C. CHOU and R. H. TOLAND, Experimental study of multiple interior impacts. *Expl Mech.* **17**, 201–206 (1977).
20. R. DIPERSIO and J. SIMON, Resistance of solid homogeneous targets to shaped charge jet penetration. Ballistic Research Laboratory Report No. 1417 (1968).
21. A. B. MERENDINO and R. VITALI, The penetration of shaped charge jets into steel and aluminum targets of various strengths. Ballistic Research Laboratory Memorandum Report No. 1932 (1968).
22. J. SIMON and R. DIPERSIO, Experimental verification of standoff effects on shaped charge jet cutoff in solid targets. Ballistic Research Laboratory Memorandum Report No. 1976 (1969).
23. R. DIPERSIO and J. SIMON, The effect of hardness on the penetration capability of shaped charge jets. Ballistic Research Laboratories Report No. 1408 (1968).
24. R. DIPERSIO, J. SIMON and A. B. MERENDINO, Shaped charge warhead performance, Part I—Experimental Observations, J. SIMON and Part II—Mathematical Relationships, R. DIPERSIO. *Proc. 4th Warhead Res. Symp.*, TP No. 3984 Naval Weapons, held at the Naval Ordnance Test Station, China Lake, California (1965).
25. J. SIMON, R. DIPERSIO and A. B. MERENDINO, Shaped charge warhead performance (II). *Proc. 5th Warhead Res. Symp.*, held at the Naval Weapons Center, China Lake, California (1967), NWC-TP 4446 (1967).
26. J. SIMON and R. DIPERSIO, The effect of target density and hardness on the penetration capability of precision shaped charge warheads. *Proc. 3rd Symp. Lightweight Armor Materials*, held in Cleveland, Ohio (1968), Sponsored by U.S. Army Materials and Mechanics Research Center, Watertown, Massachusetts, Report No. AMMRC-MS-69-02 (1969).
27. J. N. MAJERUS and B. R. SCOTT, CUMIN: A computer code for determining certain jet/target parameters from experimental data. Ballistic Research Laboratory Technical Report ARBRL-TR-02129 (1978).
28. J. MAJERUS, V. KUCHER and J. SIMON, Influence of transverse velocity upon the penetration performance of shaped charge warheads. Ballistic Research Laboratory Memorandum Report, ARBRL-MR-2742 (1977).
29. S. B. SEGLETES, A model of the effects of transverse velocity on the penetration of shaped-charge jets. Ballistic Research Laboratory Memorandum Report ARBRL-MR-3409 (1984).
30. S. B. SEGLETES, Drift velocity computations for shaped-charge jets. Ballistic Research Laboratory Memorandum Report ARBRL-MR-03306 (1983).
31. M. HELD, Characterizing shaped charge performance by stand-off behavior. *Proc. 7th Int. Symp. Ballistics*, The Hague, The Netherlands (1983).
32. R. C. GOLESWORTHY, The effect of transverse velocity on shaped charge performance. *Proc. of 7th Int. Symp. Ballistics*, The Hague, The Netherlands (1983).
33. J. CARLEONE, P. C. CHOU, W. J. FLIS and C. TANZIO, User's manual for DESC-2. Dyna East Corporation Technical Report, DETR-75-4, Revision 3 (1982).
34. J. SMITH, Shaped charge penetration at long standoff. Air Force Armament Laboratory Report No. AFATL-TR-81-25 (1981).
35. A. TATE, A theory for the deceleration of long rods after impact. *J. Mech. Phys. Solids* **15**, 387–399 (1967).
36. M. ZAID, An analytical approach to hypervelocity impact mechanics. *Hypervelocity Impact*, Fourth Symposium, APGC-TR-60-39 (1960).
37. W. P. WALTERS and J. N. MAJERUS, Impact models for penetration and hole growth. Ballistic Research Laboratory Technical Report ARBRL-TR-02069 (1978).

38. J. N. MAJERUS, W. P. WALTERS and G. P. NEITZEL, Impact models for penetration and hole growth. *Proc. 4th Int. Symp. Ballistics*, Monterey, California (1978).
39. W. P. WALTERS and J. N. MAJERUS, Hypervelocity impact models for hole growth and geometry. *Proceedings 3rd Annual Vulnerability/Survivability Symp.*, ADPA, Naval Amphibious Base, Coronada, California (1977).
40. J. N. MAJERUS and W. P. WALTERS, Axial penetration and radial growth for kinetic energy and shaped charge jet penetrators. *Proc. DEA-G-1060 Ballistic Research and Development Meeting*, Naval Surface Weapons Center, Dahlgren, Virginia, 1978, also published in the TTCP-TPW-1 Kinetic Energy Ammunition Conference, Ballistic Research Laboratory (1978).
41. W. P. WALTERS and J. N. MAJERUS, Shaped charge penetration model, Part I: Monolithic penetration and comparison with experimental data. Ballistic Research Laboratory, Technical Report ARBRL-TR-02184, AD B041747 (1979).
42. J. N. MAJERUS and W. P. WALTERS, A predictive penetration model utilizing an effective-flow viscosity of the interaction region. *Proc. 6th Int. Symp. Ballistics*, ADPA (1981).
43. W. P. WALTERS, J. N. MAJERUS and G. P. NEITZEL, Developing target armor using a jet penetration model. *Proc. 4th Vulnerability/Survivability Symp.*, Tyndall AFB, Florida (1979).
44. T. SZENDREI, Analytical model of crater formation by jet impact and its application to calculation of penetration curves and hole profiles. *Proc. 7th Int. Symp. Ballistics*, The Hague, The Netherlands (1983).
45. W. M. EVANS and A. R. UBBELOHDE, Some kinematic properties of Munroe jets. *Res. Suppl.* 3–8 (1950).
46. W. M. EVANS and A. R. UBBELOHDE, Formation of Munroe jets and their action on massive targets. *Res. Suppl.* 3–7 (1950).
47. G. LUTTWAK, Y. KIVITY and A. ABETSER, Effects of a hypervelocity jet on a layered target. *Int. J. Engng Sci.* **20**, 946–961 (1982).
48. G. ANDERSSON, L. HOLMBERG and I. MELLGARD, Experimental study of the penetration mechanisms of hollow charge jets in nonmetallic target materials. *Proc. 7th Int. Symp. Ballistics*, The Hague, The Netherlands (1983).
49. A. YA. SAGOMONYAN, *Penetration of Solids Into Compressed Continuous Media.* Moscow University (1974). Translated by DARPA (1980).
50. M. J. MURPHY, Shaped charge penetration in concrete: A unified approach. Doctoral dissertation, University of California, Davis, also UCRL-53393 and DE 83009181 (1983).
51. V. P. ALEKSEEVSKII, Penetration of a rod into a target at high velocity. *Fizika Goreniya i Vrzyva* **2**, 99–106 (1966).
52. N. S. SANASARYAN, Penetration of a cumulative jet into a barrier. *Izvestiya Akademii Nauk SSSR, Mekhanika Zhidkosti i Gaza* **6**, 151–154 (1975).
53. A. YA. SAGOMONYAN, Plate piercing by a slender solid projectile. *Vestnik Moskovskogo Universiteta, Seriya 1, Matematika, Mekhenika* **6**, 104–111, FSTC-HT-1065-81 (1975).
54. A. YA. SAGOMONYAN, Penetration of solids after high speed impact. In *Penetration of Solids Into Compressed Continuous Media*, Chap. 3. UDC 534.26 and 539.374 (1978).
55. A. YA. SAGOMONYAN, The penetration of an obstacle by a cylindrical object. *Vistnik Moskovskogo un-ta, Seriya Matematika, Mekhanika* **5**, 111–118, Izd-vo Mosk. un-ta (1977).
56. B. S. HAUGSTAD, Compressibility effects in shaped charge jet penetration. *J. appl. Phys.* **52**, 1243–1246 (1981).
57. B. S. HAUGSTAD and O. S. DULLUM, Finite compressibility in shaped charge jet and long rod penetration—the effect of shocks. *J. appl. Phys.* **52**, 5066–5071 (1981).
58. W. J. FLIS and P. C. CHOU, Penetration of compressible materials by shaped-charge jets. *Proc. 7th Int. Symp. Ballistics*, The Hague, The Netherlands (1983).
59. J. J. WHITE, M. J. WAHLL and J. E. BACKOFEN, Observation of compressibility-related effects in shaped-charge jet penetration. *J. appl. Phys.* **53**, 4515–4517 (1982).
60. J. J. WHITE and M. J. WAHLL, Shaped charge jet interactions with liquids. *Proc. 6th Int. Symp. Ballistics*. ADPA, Orlando, Florida (1981).
61. M. C. CHICK, R. B. FREY, J. J. TRIMBLE and A. BINES, Jet penetration in plexiglas. *Proc. 8th Int. Symp. Ballistics*, Orlando, Florida (1984).
62. C. P. WOIDNECK, Rod penetration in liquids. *Proc. 9th Int. Symp. Ballistics*, Shriveham, U.K. (1986).
63. P. C. CHOU, E. HIRSCH and W. P. WALTERS, The virtual origin approximation of shaped charged jets. *Proc. 6th Int. Symp. Ballistics*, Orlando, Florida (1981).
64. J. FOSTER, Integrated flash radiograph analysis—an approach to studying time-dependent phenomena in the explosive formation and projection of metals. *Proc. 7th Annual Technical Meeting Phys. Explos.*, Livermore, California (1981).
65. W. A. ALLEN and J. W. ROGERS, Penetration of a rod into a semi-infinite target. *J. Franklin Inst.* **272**, 275–284 (1961).
66. D. R. CHRISTMAN and J. W. GEHRING, Analysis of high-velocity projectile penetration mechanics. *J. appl. Phys.* **37**, 1579–1587 (1966).
67. J. R. DOYLE and R. L. BUCHHOLZ, Design, development, fabrication and testing program to demonstrate feasibility of the mass focus/fragmentation warhead. Honeywell Technical Report AFATL-TR-73-187 (1973).
68. A. TATE, Further results in the theory of long rod penetration. *J. Mech. Phys. Solids* **17**, 141–150 (1969).
69. A. TATE, A theory for the deceleration of long rods after impact. *J. Mech. Phys. Solids* **15**, 387–399 (1967).
70. A. TATE, A possible explanation for the hydrodynamic transition in high speed impact. *Int. J. Mech. Sci.* **19**, 121–123 (1977).

71. A. TATE, A simple estimate of the minimum target obliquity required for the ricochet of a high speed long rod projectile. *J. Phys. D: appl. Phys.* **12**, 1825–1829 (1979).
72. A. TATE, Long rod penetration models—Part I. A flow field model for high speed long rod penetration. *Int. J. Mech. Sci.* **28**, 535–548 (1986).
73. A. TATE, Long rod penetration models—Part II. Extensions to the hydrodynamic theory of penetration. *Int. J. Mech. Sci.* **28**, 599–612 (1986).
74. W. J. FLIS, RODPEN, a one-dimensional computer code for penetration calculations. Dyna East Corp. Technical Report No. DE-TR-79-2 (1979).
75. C. DU PONT DONALDSON, R. CONTILIANO and C. SWANSON, The qualification of target materials using the integral theory of impact. Aeronautical Research Associates of Princeton Report 295 (1976).
76. R. M. CONTILIANO, T. B. MCDONOUGH and C. V. SWANSON, Application of the integral theory of impact to the qualification of materials and the development of a simplified rod penetrator model. ARAP Report No. 368 (1978).
77. V. HOHLER and A. J. STILP, Penetration of steel and high density rods in semi-infinite steel targets. *Proc. 3rd Int. Symp. Ballistics*, Karlsruhe, Germany (1977).
78. D. A. MATUSKA, A model for high velocity penetration. *Proc. ARO Workshop on Computational Aspects of Penetration Mech.*, Aberdeen Proving Ground, Maryland (1982).
79. V. I. BELYAYEV, V. I. KOVALEVSKIY, G. V. SMIRNOV and V. A. CHOKAN, High speed deformation of metals. (*Vysokoskorostnaya Deformatsiya Metalov.*) *Nauka i Tekhnika, Minsk* (1976).
80. G. WEIHRAUCH, The behavior of copper pins upon impacting various materials at velocities of 50–1650 m s^{-1}. Dissertation, Karlsruhe University, Mechanical Engineering (1971).
81. G. D. CLARK, Study of kinetic energy penetration of multi-layered targets. M.S. Thesis, Air Force Institute of Technology, AFIT/GAE/AA/83S-1 (1983).
82. J. DEHN, The particle dynamics of target penetration. Ballistic Research Laboratory Technical Report ARBRL-TR-02188 (1979).
83. W. A. ALLEN, E. B. MAYFIELD and H. L. MORRISON, Dynamics of a projectile penetrating sand. *J. appl. Phys.* **28**, 370–376 (1957).
84. T. W. WRIGHT, A survey of penetration mechanics for long rods. Ballistic Research Laboratory Technical Report ARBRL-TR-02496 (1983).
85. M. E. BACKMAN and W. GOLDSMITH, The mechanics of penetration of projectiles into targets. *Int. J. Engng Sci.* **16**, 1–99 (1978).
86. W. GOLDSMITH, *Impact—The Theory and Physical Behavior of Colliding Solids*. Edward Arnold, London (1960).
87. W. JOHNSON, *Impact Strength of Materials*. Arnold, New York (1970).
88. G. H. JONES and J. A. ZUKAS, Mechanics of penetration: analysis and experiment. *Int. J. Engng Sci.* **16**, 879–903 (1978).
89. G. H. JONAS and J. A. ZUKAS, Armor penetration: Theory and experiment. *Proc. 14th Annual Meeting Soc. of Engng Sci.*, Lehigh University, Pennsylvania (1977).
90. J. A. ZUKAS, Impact dynamics: Theory and experiment. Ballistic Research Laboratory Technical Report ARBRL-TR-02271 (1980), also Impact dynamics, in *Emerging Technologies in Aerospace Structures, Design, Structural Dynamics and Materials* (Edited by J. R. VINSON). ASME, New York (1980).
91. J. A. ZUKAS, T. NICHOLAS, H. F. SWIFT, L. B. GRESZCZUK and D. R. CURRAN, *Impact Dynamics*, Wiley, New York (1982).
92. P. C. CHOU and W. J. FLIS, Recent developments in shaped charge technology. *Propellants, Explos., Pyrotechnics* **11**, 99–114 (1986).
93. J. T. DEHN, A unified theory of penetration. Ballistic Research Laboratory Technical Report BRL-TR-2770 (1986).